



A Journal of the Gesellschaft Deutscher Chemiker

# Angewandte Chemie

GDCh

International Edition

www.angewandte.org

## Accepted Article

**Title:** Engineered biosynthesis of  $\beta$ -alkyl tryptophan analogs

**Authors:** Christina E. Boville, Remkes A. Scheele, Philipp Koch, Sabine Brinkmann-Chen, Andrew R. Buller, and Frances H. Arnold

This manuscript has been accepted after peer review and appears as an Accepted Article online prior to editing, proofing, and formal publication of the final Version of Record (VoR). This work is currently citable by using the Digital Object Identifier (DOI) given below. The VoR will be published online in Early View as soon as possible and may be different to this Accepted Article as a result of editing. Readers should obtain the VoR from the journal website shown below when it is published to ensure accuracy of information. The authors are responsible for the content of this Accepted Article.

**To be cited as:** *Angew. Chem. Int. Ed.* 10.1002/anie.201807998  
*Angew. Chem.* 10.1002/ange.201807998

**Link to VoR:** <http://dx.doi.org/10.1002/anie.201807998>  
<http://dx.doi.org/10.1002/ange.201807998>

# Engineered biosynthesis of $\beta$ -alkyl tryptophan analogs

Christina E. Boville<sup>+</sup>, Remkes A. Scheele<sup>+</sup>, Philipp Koch, Sabine Brinkmann-Chen, and Andrew R. Buller<sup>\*</sup>, Frances H. Arnold<sup>\*</sup>

**Abstract:** Non-canonical amino acids (ncAAs) with dual stereocenters at the  $\alpha$  and  $\beta$  positions are valuable precursors to natural products and therapeutics. Despite the potential applications of such bioactive  $\beta$ -branched ncAAs, their availability is limited due to the inefficiency of the multi-step methods used to prepare them. Here we report a stereoselective biocatalytic synthesis of  $\beta$ -branched tryptophan analogs using an engineered variant of *Pyrococcus furiosus* tryptophan synthase (*Pf*TrpB), *Pf*TrpB<sup>7E6</sup>. *Pf*TrpB<sup>7E6</sup> is the first biocatalyst to synthesize bulky  $\beta$ -branched tryptophan analogs in a single step, with demonstrated access to 27 ncAAs. The molecular basis for the efficient catalysis and broad substrate tolerance of *Pf*TrpB<sup>7E6</sup> was explored through X-ray crystallography and UV-visible light spectroscopy, which revealed that a combination of active-site and remote mutations increase the abundance and persistence of a key reactive intermediate. *Pf*TrpB<sup>7E6</sup> provides an operationally simple and environmentally benign platform for preparation of  $\beta$ -branched tryptophan building blocks.

Amino acids are nature's building blocks for bioactive molecules. Alongside the standard proteinogenic amino acids are diverse non-canonical amino acids (ncAAs) that are structurally similar but are not ribosomally incorporated into proteins. Due to the presence of functional groups that confer novel chemical and biological properties,<sup>[1]</sup> ncAAs can be found in natural products and 12% of the 200 top-grossing pharmaceuticals.<sup>[2,3]</sup> Of interest are  $\beta$ -branched ncAAs, which possess a chiral center at the  $\beta$ -position in addition to the standard chirality at the  $\alpha$ -position of an amino acid (Figure 1a). The two adjacent stereocenters impose conformational constraints that affect the biochemical properties of both the amino acids themselves and the molecules they compose.<sup>[4-7]</sup> These properties make  $\beta$ -branched ncAAs frequent components of useful natural products, biochemical probes, and therapeutics (Figure 1b).<sup>[8-10]</sup> Despite their broad utility, most  $\beta$ -branched ncAAs are not readily available due to the challenge of forming two adjacent stereocenters while tolerating the reactive functional groups present in amino acids.<sup>[11-13]</sup> For example, traditional organic synthesis of (2*S*, 3*S*)- $\beta$ -methyltryptophan ( $\beta$ -MeTrp) requires multiple steps that incorporate protecting groups, hazardous reagents, and expensive metal catalysts.<sup>[14]</sup> To take full advantage of these bioactive molecules, an improved methodology is needed to synthesize  $\beta$ -branched ncAAs.

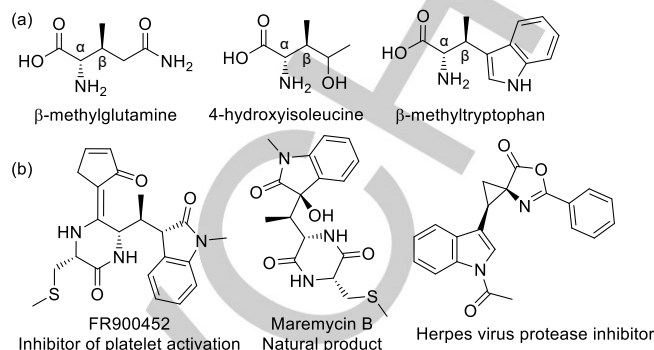


**Figure 1.** Representative  $\beta$ -branched amino acids. (a) Examples of  $\beta$ -branched ncAAs. (b) Examples of products derived from  $\beta$ -branched tryptophan analogs.

Enzymes offer an efficient and sustainable alternative to chemical synthesis and are routinely used to generate enantiopure amino acids from simple materials without protecting groups.<sup>[15]</sup> Although several classes of enzymes have been employed in this pursuit, those using the pyridoxal phosphate cofactor (PLP, vitamin B6) are among the most prominent.<sup>[16]</sup> The most common biocatalytic route to an amino acid requires a preassembled carbon skeleton and uses a PLP-dependent transaminase to set the stereochemistry. However, as with traditional organic methodologies, enzymatic synthesis of  $\beta$ -branched ncAAs is often confounded by the presence of a second stereocenter. The capacity to incorporate biocatalytic C–C bond-forming steps *en route* to diverse  $\beta$ -branched ncAAs would therefore be a powerful synthetic tool.

Few  $\beta$ -branched ncAA synthases have been reported, and even more rare are enzymes that produce branches larger than a methyl group. We previously engineered the  $\beta$ -subunit of the PLP-dependent enzyme tryptophan synthase from *Pyrococcus furiosus* (*Pf*TrpB) as a stand-alone ncAA synthase able to generate tryptophan (Trp) analogs from serine (Ser) and the corresponding substituted indole (Figure 2a).<sup>[17-19]</sup> Further engineering for improved C–C bond formation with indole analogs and threonine (Thr) led to *Pf*TrpB<sup>2B9</sup> (eight mutations from wild-type *Pf*TrpB), which exhibited a >1,000-fold improvement in (2*S*, 3*S*)- $\beta$ -methyltryptophan ( $\beta$ -MeTrp) production relative to wild type (Figure 2b).<sup>[20,21]</sup> While the reactive amino-acrylate intermediate (E(A-A)) (Figure 3a) readily forms with Thr, mechanistic analysis showed that competing hydrolysis of (E(A-A)) resulted in abortive deamination that consumed the amino acid substrate (Figure 3b),<sup>[22]</sup> limiting the enzyme's yield (typically < 50%) with a single equivalent of Thr. Later, the full tryptophan synthase complex was explored as a  $\beta$ -branched ncAA synthase.<sup>[10]</sup> While multiple  $\beta$ -MeTrp analogs were reported using this system, other  $\beta$ -alkyl tryptophan analogs remained out of reach.

To surmount these challenges, we sought to identify mutations that would facilitate formation of E(A-A) with the more challenging (2*S*, 3*R*)- $\beta$ -ethylserine ( $\beta$ -EtSer) and (2*S*, 3*R*)- $\beta$ -

[a] Dr. C. E. Boville, R. A. Scheele, P. Koch, Dr. S. Brinkmann-Chen, Prof. F. H. Arnold  
Division of Chemistry and Chemical Engineering 210-41, California Institute of Technology, 1200 East California Boulevard, Pasadena, California 91125, United States  
Email: frances@cheme.caltech.edu

[b] Prof. A. R. Buller  
Department of Chemistry, University of Wisconsin, 1101 University Avenue, Madison, WI 53706, United States  
Email: arbuller@wisc.edu

[+ ] These authors contributed equally to this work.  
Supporting information for this article is given via a link at the end of the document.

## COMMUNICATION

WILEY-VCH

propylserine ( $\beta$ -PrSer) substrates while simultaneously decreasing E(A-A) hydrolysis (Figure 2c). The latter is essential, as increasingly bulky alkyl chains are thought to hinder nucleophilic attack. Increased E(A-A) persistence will allow more time for the intrinsically slower addition reaction to occur while reducing the amount of starting material lost to competing hydrolysis (Figure 3b).

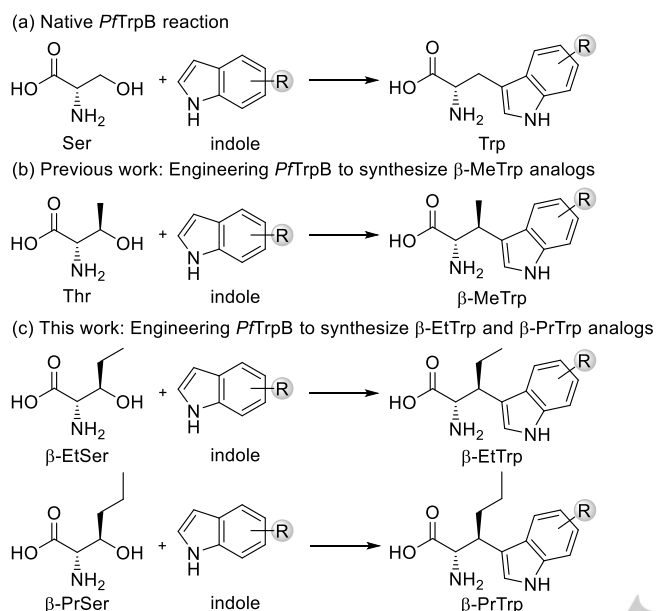


**Figure 2.** Synthesis of Trp and Trp analogs by *PflTrpB*.

We chose *PflTrpB*<sup>2B9</sup> as the parent for evolution to increase production of  $\beta$ -EtTrp. *PflTrpB*<sup>2B9</sup> was sluggish with  $\beta$ -EtSer (80 total turnovers, TTN) and gave too little signal for high-throughput screening.<sup>[17]</sup> Speculating that active-site mutations would promote the formation of E(A-A) with larger, sterically demanding  $\beta$ -substituents, we used a structure-guided approach to improve activity with  $\beta$ -EtSer. Modeling  $\beta$ -EtSer into the *PflTrpB*<sup>2B9</sup> active site as E(A-A) (PDB: 5VM5)<sup>[23]</sup> suggested a steric clash with L161 (Figure 4a). Hypothesizing that this constraint could be reduced by mutating L161 to a residue with a smaller side chain, we expressed and assayed variants *PflTrpB*<sup>2B9</sup> L161V, L161A, and L161G. We found that L161V and L161A increased the TTN 14-fold and 10-fold, respectively, whereas L161G decreased activity by a factor of 2.6 (Figure 4b). As our long-term interest is to produce a catalyst that accommodates a wider range of  $\beta$ -alkyl chains, we selected *PflTrpB*<sup>2B9</sup> L161A as the parent enzyme for directed evolution, with the rationale that the smaller sidechain of alanine would minimize steric clashes with bulkier substrates.

We then introduced random mutations into the *PflTrpB*<sup>2B9</sup> L161A gene and screened for (2S, 3S)- $\beta$ -ethyltryptophan ( $\beta$ -EtTrp) at 290 nm under saturating substrate conditions.<sup>[17]</sup> Screening of 352 variants yielded *PflTrpB*<sup>0E3</sup> (L91P), which displayed a 43-fold increase in TTN for  $\beta$ -EtTrp (Figure 4c). *PflTrpB*<sup>0E3</sup> was then used to parent a second round of random mutagenesis, yielding variant *PflTrpB*<sup>8C8</sup> (V173E), which improved  $\beta$ -EtTrp yields 54-fold relative to *PflTrpB*<sup>2B9</sup>. We then recombined mutations in TrpB<sup>8C8</sup>, allowing each residue to retain the mutation or revert to wild type. Recombination included all

residues except those crucial for starting activity with Ser (T292S), Thr (F95L), and  $\beta$ -EtSer (L161A and L91P) (Table S1). Recombination also included F274L, which was previously identified as an activating mutation.<sup>[17]</sup> Screening revealed that I68V and T321A were non-essential mutations, but that F274L was beneficial, yielding variant *PflTrpB*<sup>7E6</sup>. *PflTrpB*<sup>7E6</sup> showed comparable stability (Table S2) and a modest increase in activity (58-fold improvement relative to *PflTrpB*<sup>2B9</sup>, Figure 4c). Another round of recombination sampled previously identified mutations Q38R, M139L, N166D, and S335N and allowed for reversion of L91P.<sup>[18]</sup> This yielded *PflTrpB*<sup>2G8</sup> (see Table S3) with slightly lower activity than *PflTrpB*<sup>7E6</sup>. *PflTrpB*<sup>7E6</sup> was selected for mechanistic characterization as it is a simple catalyst with excellent activity and is amenable to crystallization.

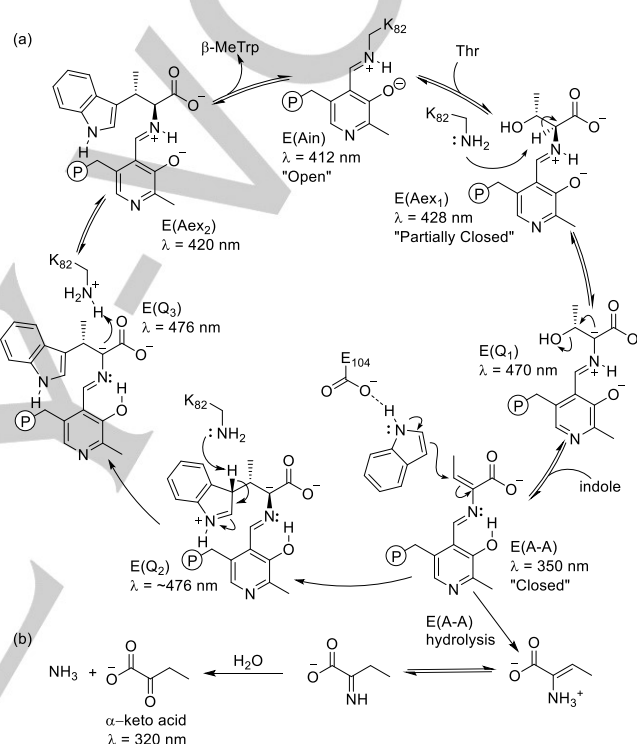


**Figure 3.** The putative catalytic cycle for *PflTrpB* synthesizing  $\beta$ -MeTrp. (a) The catalytic cycle with the expected UV-vis peaks (b) E(A-A) may also undergo a kinetically competing hydrolysis reaction to generate  $\alpha$ -keto acids.

We sought to identify which evolved properties enabled increased TTNs with challenging  $\beta$ -branched substrates. As described above, the activity and substrate scope of the parent enzyme, *PflTrpB*<sup>2B9</sup>, were limited by low steady-state population (abundance) and subsequent breakdown (persistence) of the reactive E(A-A) intermediate.<sup>[21]</sup> To assess the abundance of E(A-A), we capitalized on the intrinsic spectroscopic properties of the PLP cofactor to visualize the steady-state distribution of intermediates throughout the catalytic cycle (Figure 3a).<sup>[24]</sup> With the addition of  $\beta$ -EtSer to *PflTrpB*<sup>7E6</sup>, the internal aldimine peak (E(Ain), 412 nm) decreased and E(A-A) (350 nm) became the major species (Figure 4d). This is a notable change, as when  $\beta$ -EtSer was added to *PflTrpB*<sup>2B9</sup>, the external aldimine (E(Aex<sub>1</sub>), 428 nm) accumulated and no E(A-A) was observed. To assess the persistence of E(A-A), we assayed the deamination rate of *PflTrpB*<sup>7E6</sup> and saw up to a 4-fold decrease in the deamination reaction relative to *PflTrpB*<sup>2B9</sup> (Table S4). We then probed the

## COMMUNICATION

WILEY-VCH

enzyme's coupling efficiency under reaction conditions where product formation is limited only by the consumption of starting material through the competing deamination reaction. We observed an increase in product formation from 5% with *PfTrpB*<sup>2B9</sup> to 96% with *PfTrpB*<sup>7E6</sup> when  $\beta$ -EtSer was the substrate (Figure 4c). Collectively, these data indicate that increased product formation was achieved by incorporating mutations that facilitate the formation of E(A-A) and increase its lifetime in the active site.

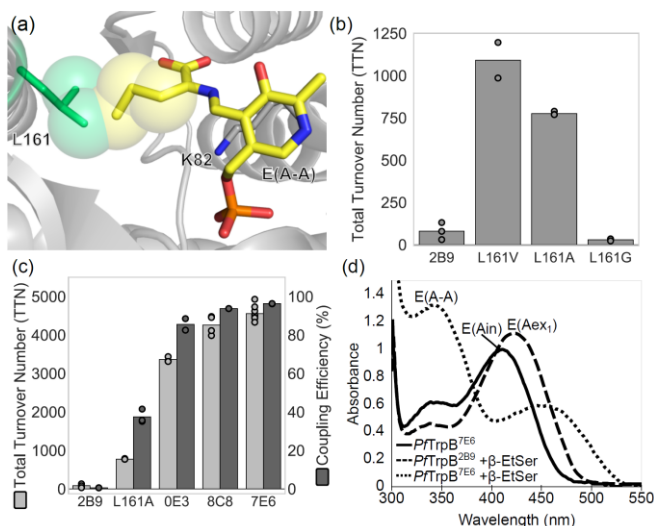


**Figure 4.** Engineering *PfTrpB* for  $\beta$ -EtTrp synthesis. (a)  $\beta$ -EtSer as E(A-A) (yellow) modeled in the *PfTrpB*<sup>2B9</sup> (PDB: 5VM5, gray) active site with L161 (green). Spheres represent the Van der Waals radii. (b)  $\beta$ -EtTrp production by *PfTrpB*<sup>2B9</sup> with L161V, L161A, or L161G mutations. (c)  $\beta$ -EtTrp production and coupling efficiency by engineered *PfTrpB* variants. Bars represent the average of all data points, with individual reactions shown as circles. (d) The steady-state population of *PfTrpB*<sup>7E6</sup> and *PfTrpB*<sup>2B9</sup> with  $\beta$ -EtSer as determined by UV-visible light spectroscopy.

*PfTrpB*<sup>7E6</sup> has only a single mutation in the active site (Figure S1); the other eight beneficial mutations are distributed throughout the protein.<sup>[17,25]</sup> Remote mutations may be affecting the enzyme's conformational dynamics, which have been previously shown to be linked to the catalytic cycle of *PfTrpB* (Figure 3a).<sup>[22,23,25,26]</sup> To examine the state of the *PfTrpB*<sup>7E6</sup> active site and its connection to the COMM domain conformational cycling, we determined the X-ray crystal structures of *PfTrpB*<sup>7E6</sup> in the E(Ain) state and with  $\beta$ -EtSer bound in the active site as E(A-A).

Earlier *PfTrpB* variants, including *PfTrpB*<sup>2B9</sup>, were nearly identical to wild-type *PfTrpB* (PDB: 5DVZ) in the open state.<sup>[17,23]</sup> Here, the 2.26-Å structure of *PfTrpB*<sup>7E6</sup> (PDB: 6CUV) shows preorganization toward a more closed conformation. Specifically, in half of the protomers, the COMM domain has shifted into a distinct partially-closed conformation that was previously associated with substrate binding (Figure 5a). While many residues may contribute to the stabilization of this state, we hypothesize that the mutation L91P destabilizes open states. This residue lies on an  $\alpha$ -helix immediately prior to the COMM domain in the sequence and causes a kink in the helix that shifts the structure toward more closed states (Figure 5b).

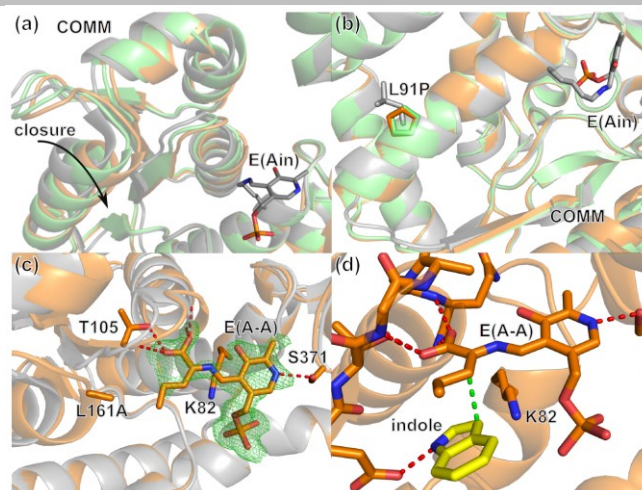


**Figure 5.** Substrate binding and conformational changes in *PfTrpB*. (a) The COMM domain of *PfTrpB* undergoes rigid body motion. Shown are wild-type *PfTrpB* (PDB: 5DVZ, gray), *PfTrpB*<sup>7E6</sup> (PDB: 6CUV, green), and  $\beta$ -EtSer-bound *PfTrpB*<sup>7E6</sup> as E(A-A) (PDB: 6CUV, orange). (b) The mutation L91P introduces a kink in the  $\alpha$ -helix adjacent to the COMM domain. (c)  $\beta$ -EtSer bound to *PfTrpB*<sup>7E6</sup> as E(A-A) is shown with  $F_o-F_c$  map contoured at  $2.0\sigma$  (green). The delta carbon of the amino-acrylate is not well resolved. Hydrogen bonds are shown as red dashes. (d) Indole (yellow) modeled in the active site of *PfTrpB*<sup>7E6</sup> with  $\beta$ -EtSer as E(A-A). The green dash links the bond-forming atoms.

We next soaked *PfTrpB*<sup>7E6</sup> with  $\beta$ -EtSer and obtained a 1.75-Å structure with  $\beta$ -EtSer bound as E(A-A) in two protomers (PDB: 6CUZ). As expected, the COMM domain underwent rigid-body motion to the closed conformation (Figure 5a) where the steric complementarity between the longer  $\beta$ -alkyl chain and L161A becomes apparent. Notably, the L161A mutation does not appear to induce significant alterations elsewhere in the active site (Figure 5c). When indole is modeled into the active site, there is space to accommodate even longer  $\beta$ -branched substituents as well as a range of indole nucleophiles (Figure 5d).

As our goal was to evolve a versatile  $\beta$ -branched ncAA synthase, we next explored the substrate scope of *PfTrpB*<sup>7E6</sup>. If improvements in activity came through increased stability of E(A-A), the same mutations should increase activity with multiple amino acid substrates. Indeed, we found that although we screened for  $\beta$ -EtTrp synthesis,  $\beta$ -MeTrp and (2S, 3S)- $\beta$ -propyltryptophan ( $\beta$ -PrTrp) synthesis were simultaneously improved 3.6-fold and 36-fold, respectively (Figure 6a). Further, directed evolution improved the enzyme's coupling efficiency (Figure 6b) and amino-acrylate formation (Figure 6c-d) with all three acid substrates. Next, we revisited our earlier hypothesis that the L161V mutation would clash with larger substrates and observed that the TTN for  $\beta$ -PrTrp formation was reduced 5-fold (Figure S2a). In addition, *PfTrpB*<sup>7E6</sup> retained the robust Trp activity that is the hallmark of the wild-type enzyme (Figure S2b), demonstrating that the L161A mutation permitted catalysis with four different amino acid substrates.

*PfTrpB*<sup>7E6</sup> showed only trace activity with (2S)- $\beta$ -isopropylserine ( $\beta$ -iPrSer). To understand why catalysis did not proceed with this bulkier sidechain, we soaked  $\beta$ -iPrSer into *PfTrpB*<sup>7E6</sup> crystals and obtained a 1.77-Å structure (PDB: 6CUT), which shows the catalytically unreactive (2S, 3S) diastereomer of  $\beta$ -iPrSer bound as E(Aex<sub>1</sub>) (Figure S3). Though (2S, 3S)- $\beta$ -

## COMMUNICATION

WILEY-VCH

iPrSer can form E(Aex<sub>1</sub>), dehydration across the C<sub>α</sub>-C<sub>β</sub> bond requires a rotameric shift of the side chain that is potentially hindered by steric interactions with an adjacent loop.<sup>[27]</sup> Further work is needed to understand whether the poor activity of *Pf*TrpB<sup>7E6</sup> with (2*S*, 3*R*)-β-iPrSer reflects inhibition by an isomeric analog, increased allylic strain of the amino-acrylate, or a combination of effects.

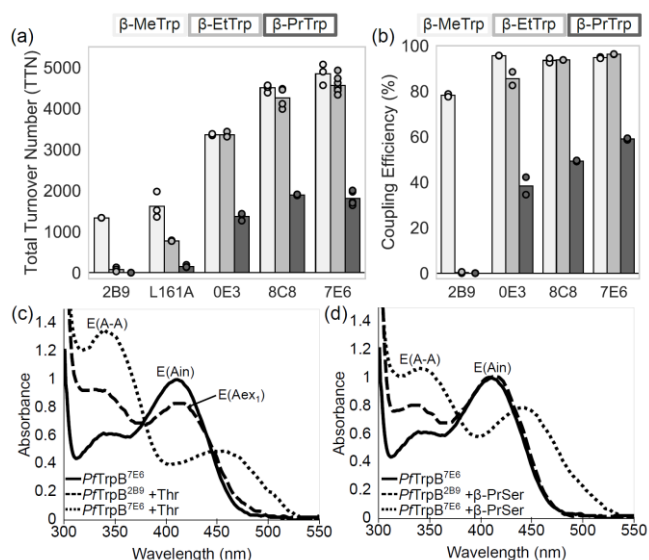


**Figure 6.** *Pf*TrpB engineering grants access to a range of β-branched tryptophan analogs. (a) TTN of *Pf*TrpB with β-MeTrp, β-EtTrp, and β-PrTrp. Bars represent the average of all data points, with individual reactions shown as circles. At minimum, reactions were performed in duplicate. (b) Variant coupling efficiency with Thr, β-EtSer, and β-PrSer. (c-d) The steady-state population of *Pf*TrpB<sup>7E6</sup> and *Pf*TrpB<sup>2B9</sup> with (c) Thr or (d) β-PrSer as determined by UV-visible light spectroscopy.

In addition to acting on multiple amino acid substrates, we hypothesized that *Pf*TrpB<sup>7E6</sup> would retain the wild-type enzyme's breadth of reactivity with indole analogs.<sup>[17–19]</sup> We performed analytical biotransformations with 11 representative nucleophiles and three β-branched amino acid substrates, yielding 27 tryptophan analogs, 20 of which are previously unreported (Table 1). Each reaction was analyzed by liquid-chromatography/mass spectrometry (LCMS), and TTNs were calculated by comparing product and substrate absorption at the isosbestic wavelength (Table S5). We found that methyl- and halogen-substituted indole analogs remained well-tolerated by

*Pf*TrpB<sup>7E6</sup>. We also observed activity with 5-chloroindole and Thr, a reaction that was undetectable for the parent enzyme, *Pf*TrpB<sup>2B9</sup>. In addition, we abolished the undesirable *N*-alkylation reaction that occurred with *Pf*TrpB<sup>2B9</sup> in the presence of 7-azaindole and 4-fluoroindole.<sup>[21]</sup> However, yields with *N*-nucleophilic substrates such as indazole remained low with β-branched substrates relative to Ser. Importantly, *Pf*TrpB<sup>7E6</sup> can synthesize these ncAAs using only a single equivalent of the amino acid substrate, whereas *Pf*TrpB<sup>2B9</sup> had required 10 equivalents. This is a testament to the value of improving the stability of the reactive E(A-A) intermediate.

All product identities were confirmed by <sup>1</sup>H- and <sup>13</sup>C-NMR as well as high-resolution mass spectrometry from 100-μmol preparative reactions. Reactions used two equivalents of amino acid substrate and 0.01 to 0.4 mol% catalyst loading, and under these conditions *Pf*TrpB<sup>7E6</sup> maintained robust activity: β-MeTrp (6,600 TTN, 88% yield), β-EtTrp (6,200 TTN, 82% yield), and β-PrTrp (2,100 TTN, 84% yield). We also used *Pf*TrpB<sup>2G8</sup> (Table S3) to synthesize and characterize 27 tryptophan analogs on a preparative scale (Table S6). Reactions may be further optimized by tuning catalyst loading and increasing substrate equivalents (Table S7).

In conjunction with the high expression levels of *Pf*TrpB<sup>7E6</sup> (~300 mg enzyme per L culture), a range of β-branched ncAAs are now accessible on a preparative scale. We have developed a new biocatalytic route to (2*S*, 3*S*)-tryptophan analogs using the engineered thermostable catalyst, *Pf*TrpB<sup>7E6</sup>. Directed evolution increased the abundance and persistence of the key E(A-A) intermediate through the introduction of active-site and remote mutations. In turn, *Pf*TrpB<sup>7E6</sup> displays improved coupling efficiency with multiple β-branched amino acid substrates. This work significantly extends previous efforts to engineer *Pf*TrpB enzymes, which have proven to be versatile and efficient catalysts for production of tryptophan analogs.

## Acknowledgements

The authors thank Dr. David Romney, Patrick Almhjell, Dr. Christopher Prier, Nathaniel Goldberg, and Ella Watkins for helpful discussions and comments on the manuscript. We thank Dr. Jens Kaiser of the Caltech Molecular Observatory, Dr. Scott Virgil and the Center for Catalysis and Chemical Synthesis, and Dr. Mona Shahgholi and Naseem Torian from the Caltech Mass Spectrometry Laboratory. This work was funded by the Rothenberg Innovation Initiative. C.E.B. was supported by a postdoctoral fellowship from the Resnick Sustainability Institute.

**Table 1.** β-Branched tryptophan analogs synthesized by *Pf*TrpB<sup>7E6</sup>. Average TTN (10,000 max TTN) and standard deviation are indicated for each combination of amino acid and nucleophile substrate as determined by LCMS. At minimum, reactions were performed in duplicate. See Supplemental Information for experimental details. N.D. not detected.

| Electrophilic Substrate | Nucleophilic Substrate |                |                |                |                |                |                |                |                |             |          |
|-------------------------|------------------------|----------------|----------------|----------------|----------------|----------------|----------------|----------------|----------------|-------------|----------|
|                         | Indole                 | 2-methylindole | 4-methylindole | 4-fluoroindole | 5-methylindole | 5-fluoroindole | 5-chloroindole | 6-methylindole | 7-methylindole | 7-azaindole | Indazole |
| Thr                     | 4800 ± 300             | 4500 ± 300     | 1000 ± 50      | 4500 ± 200     | 800 ± 50       | 5800 ± 60      | 90 ± 20        | 1400 ± 100     | 3000 ± 100     | 4800 ± 10   | 200 ± 10 |
| β-EtSer                 | 4600 ± 200             | 3000 ± 300     | 700 ± 80       | 1600 ± 10      | 100 ± 10       | 3700 ± 400     | N.D.           | 700 ± 30       | 2800 ± 200     | N.D.        | N.D.     |
| β-PrSer                 | 1800 ± 200             | 200 ± 40       | 100 ± 20       | 200 ± 50       | 80 ± 10        | 400 ± 100      | N.D.           | 100 ± 10       | 1100 ± 100     | N.D.        | N.D.     |

## COMMUNICATION

WILEY-VCH

R.A.S. was supported by funding from the University of Groningen.

**Keywords:** amino acids • biocatalysis • amino acids • directed evolution • lyases

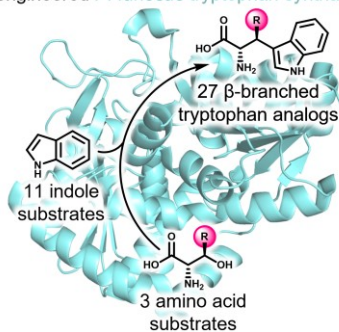
- [1] F. Agostini, J.-S. Völler, B. Kocsch, C. G. Acevedo-Rocha, V. Kubyshkin, N. Budisa, *Angew. Chem. Int. Ed.* **2017**, *56*, 9680–9703.
- [2] N. A. McGrath, M. Brichacek, J. T. Njardarson, *J. Chem. Educ.* **2010**, *87*, 1348–1349.
- [3] M. A. T. Blaskovich, *Journal of Medicinal Chemistry* **2016**, *59*, 10807–10836.
- [4] S. E. Gibson (née Thomas), N. Guillo, M. J. Tozer, *Tetrahedron* **1999**, *55*, 585–615.
- [5] V. J. Hruby, *J. Med. Chem.* **2003**, *46*, 4215–4231.
- [6] V. W. Cornish, M. I. Kaplan, D. L. Veenstra, P. A. Kollman, P. G. Schultz, *Biochemistry* **1994**, *33*, 12022–12031.
- [7] C. Haskell-Luevano, L. W. Boteju, H. Miwa, C. Dickinson, I. Gantz, T. Yamada, M. E. Hadley, V. J. Hruby, *J. Med. Chem.* **1995**, *38*, 4720–4729.
- [8] Y. Zou, Q. Fang, H. Yin, Z. Liang, D. Kong, L. Bai, Z. Deng, S. Lin, *Angew. Chem. Int. Ed.* **2013**, *52*, 12951–12955.
- [9] J. Michaux, G. Niel, J.-M. Campagne, *Chem. Soc. Rev.* **2009**, *38*, 2093.
- [10] D. Francis, M. Winn, J. Latham, M. F. Greaney, J. Micklefield, *ChemBioChem* **2017**, *18*, 382–386.
- [11] S. G. Davies, A. M. Fletcher, A. B. Frost, J. A. Lee, P. M. Roberts, J. E. Thomson, *Tetrahedron* **2013**, *69*, 8885–8898.
- [12] S.-Y. Zhang, Q. Li, G. He, W. A. Nack, G. Chen, *J. Am. Chem. Soc.* **2013**, *135*, 12135–12141.
- [13] S. Lou, G. M. McKenna, S. A. Tymonko, A. Ramirez, T. Benkovics, D. A. Conlon, F. González-Bobes, *Org. Lett.* **2015**, *17*, 5000–5003.
- [14] Y. Sawai, M. Mizuno, T. Ito, J. Kawakami, M. Yamano, *Tetrahedron* **2009**, *65*, 7122–7128.
- [15] Y.-P. Xue, C.-H. Cao, Y.-G. Zheng, *Chem. Soc. Rev.* **2018**, *47*, 1516–1561.
- [16] M. L. Di Salvo, N. Budisa, R. Contestabile, *Beilstein Bozen Symp. Mol. Eng. Control* **2012**, 27–66.
- [17] A. R. Buller, S. Brinkmann-Chen, D. K. Romney, M. Herger, J. Murciano-Calles, F. H. Arnold, *Proc. Natl. Acad. Sci. U.S.A.* **2015**, *112*, 14599–14604.
- [18] D. K. Romney, J. Murciano-Calles, J. E. Wehrmüller, F. H. Arnold, *J. Am. Chem. Soc.* **2017**, *139*, 10769–10776.
- [19] J. Murciano-Calles, D. K. Romney, S. Brinkmann-Chen, A. R. Buller, F. H. Arnold, *Angew. Chem. Int. Ed.* **2016**, *55*, 11577–11581.
- [20] A. R. Buller, P. van Roye, J. Murciano-Calles, F. H. Arnold, *Biochemistry* **2016**, *55*, 7043–7046.
- [21] M. Herger, P. van Roye, D. K. Romney, S. Brinkmann-Chen, A. R. Buller, F. H. Arnold, *J. Am. Chem. Soc.* **2016**, *138*, 8388–8391.
- [22] B. G. Caulkins, R. P. Young, R. A. Kudla, C. Yang, T. J. Bittbauer, B. Bastin, E. Hilario, L. Fan, M. J. Marsella, M. F. Dunn, et al., *J. Am. Chem. Soc.* **2016**, *138*, 15214–15226.
- [23] A. R. Buller, P. van Roye, J. K. B. Cahn, R. A. Scheele, M. Herger, F. H. Arnold, *J. Am. Chem. Soc.* **2018**, *140*, 7256–7266.
- [24] W. F. Drewe, M. F. Dunn, *Biochemistry* **1986**, *25*, 2494–2501.
- [25] M. F. Dunn, *Arch. Biochem. Biophys.* **2012**, *519*, 154–166.
- [26] B. G. Caulkins, B. Bastin, C. Yang, T. J. Neubauer, R. P. Young, E. Hilario, Y. M. Huang, C. A. Chang, L. Fan, M. F. Dunn, et al., *J. Am. Chem. Soc.* **2014**, *136*, 12824–12827.
- [27] E. W. Miles, D. R. Houck, H. G. Floss, *J. Biol. Chem.* **1982**, *257*, 14203–14210.

Accepted Manuscript

## COMMUNICATION

$\beta$ -branched tryptophan analogs are useful bioactive molecules but are challenging to synthesize. The  $\beta$ -subunit of tryptophan synthase (TrpB) was evolved to make  $\beta$ -branched tryptophan analogs readily available. This yielded a new TrpB variant, *Pf*TrpB<sup>7E6</sup>, that can synthesize 27 enantiopure  $\beta$ -branched tryptophan analogs in a single step from simple starting materials.

Biocatalytic synthesis of  $\beta$ -branched tryptophan analogs using engineered *P. furiosus* tryptophan synthase



Christina E. Boville, Remkes A. Scheele, Philipp Koch, Sabine Brinkmann-Chen, and Andrew R. Buller\*, Frances H. Arnold\*

Engineered biosynthesis of  $\beta$ -alkyl tryptophan analogs

Accepted Manuscript